Application of Wavelet Packets in Bearing Fault Diagnosis

NIKOLAOS G. NIKOLAOU, IOANNIS A. ANTONIADIS
Department of Mechanical Engineering, Machine Design and Control Systems Section
National Technical University of Athens
P.O. Box 64078, Athens 15710
GREECE

Abstract: - In this paper the wavelet packet transform is used for processing of rolling element bearing fault signals. The effectiveness of the envelope analysis technique is combined with the flexibility of the wavelet packet transform, helping in the minimization of interventions by the end user. According to the proposed method, a time-frequency decomposition of a vibration signal is provided and the components carrying the important diagnostic information are selected for further processing. The parameter selection criteria are discussed. The method is evaluated using a simulated signal and actual vibration signals measured from bearings with defects at different locations.

Key-Words: - Wavelet, Wavelet packet, Vibration, Bearing, Fault Diagnosis

1 Introduction

Bearings are among the most important and frequently encountered components in the vast majority of rotating machines, their carrying capacity and reliability being prominent for the overall machine performance. Therefore, quite naturally, fault identification of rolling element bearings has been the subject of extensive research [1].

Vibration analysis has been established as the most common and reliable analysis method. Defects or wear cause impacts at frequencies governed by the operating speed of the unit and the geometry of the bearings, which in turn are modulated by machine natural frequencies. The signature of a damaged bearing consists of exponentially decaying ringing that occurs periodically at the characteristic defect frequency. A corresponding well-established physical model has been proposed in [2]. The location dependent characteristic defect frequencies make it possible to detect the presence of a defect and to diagnose on what part of the bearing the defect is. The difficulty of defect detection lies in the fact that the signature of a defective bearing is spread across a wide frequency band and hence can be easily masked by noise. Its spectrum consists of of a series of harmonics of the characteristic defect frequency, with the highest amplitude around the resonance frequency. Typically the amplitude at the characteristic defect frequency is small and not easily noticed. For the solution of this problem several methods have been proposed, based either directly on the shape of the time domain form of the signal, or on its spectral content. Of all those methods, the most widely accepted is the envelope analysis [3-4]. The simplest method to perform envelope analysis is to pass the signal through an analogue high-pass filter to remove the low-frequency noise and then by rectifying and frequency analysing the signal, the defect frequency components can be determined in the envelope spectrum. Envelope analysis can be made more efficient by digitising the signal and band-pass filtering it in a region where there is a high signal-to-noise ratio, typically around a resonance.

The ringing modes of a bearing and its supporting structure cannot easily be predicted, because they depend on factors such as operating condition and development of the defect. Thus, in frequency domain methods, an intelligent selection of the frequency band is required.

In order to overcome this problem a number of time-frequency domain methods have been proposed, such as the Short Time Fourier Transform, the Wigner-Ville Distribution and the Wavelet Transform. Wavelets have been established as the most widespread tool in many areas of signal processing, due to their flexibility and to their efficient computational implementation [5]. They have been introduced in vibrations [6] and there are specific case studies for bearing fault detection [7-8] and for other machine components [9]. In many cases the application of wavelets has been combined and enriched by using additional features, such as Gaussian/exponential-enveloped functions [10], or de-noising methods [11].

The Wavelet Packet Transform is a generalization of the wavelet transform and has been used in signal processing for denoising or compression of signals [12-13]. Applications in machining process have also been proposed [14-15]. In this paper a method is proposed, which uses the wavelet packet transform as a systematic tool for the analysis of vibration signals resulting from bearings with localized defects. Prediction of the resonant frequencies is not required, minimizing the interventions by the end user. In chapter 2 a brief review of the basics of the Wavelet transform and the wavelet packet transform are presented. In section 3 the implementation of the proposed method is described and the major parameters affecting its performance are analyzed. Results of the implementation on a simulated signal as well as on experimental and industrial measurements for two different types of bearing faults are provided in section 4, verifying the effectiveness of the method.

2 Brief Review of the Wavelet Theory

2.1 The Wavelet Transform

The continuous wavelet transform (CWT) of a finite energy signal $x(t)$ with the analyzing wavelet $\psi(t)$ is the convolution of $x(t)$ with a scaled and conjugated wavelet:

$$W(\alpha,b) = \alpha^{-1/2}\int_{-\infty}^{\infty} s(t)\psi^*(\frac{t-b}{\alpha})dt \qquad (1)$$

The wavelet coefficient $W(\alpha,b)$ measures the similarity between the signal $s(t)$ and the analyzing wavelet $\psi(t)$ at different scales as defined by the parameter a, and different time positions as defined by the parameter b. The factor $\alpha^{-1/2}$ is used for energy preservation. Equation (1) indicates that the wavelet analysis is a time-frequency analysis, or, more properly termed, a time-scale analysis. The wavelet transform can be also considered as a special filtering operation. The frequency segmentation is obtained by translation and dilation of the analyzing wavelet. At successively larger scales the frequency resolution improves and the time resolution decreases.

The discrete wavelet transform is performed by choosing fixed values $\alpha=2^m$ and $b=n2^m$, where m,n are integers. Thus, discrete wavelets $\psi_{m,n}(t)=2^{-m/2}\psi(2^{-m}t-n)$ are constructed constituting an orthonormal basis. The discrete wavelet analysis can be implemented by the scaling filter $h(n)$, which is a lowpass filter related to the scaling function $\varphi(t)$, and the wavelet filter $g(n)$, which is a highpass filter related to the wavelet function $\psi(t)$.

$$h(n) = \frac{1}{\sqrt{2}}\langle\varphi(t),\varphi(2t-n)\rangle$$
$$g(n) = \frac{1}{\sqrt{2}}\langle\varphi(t),\varphi(2t-n)\rangle = (-1)^n h(1-n) \qquad (2)$$

The computation of these filters and their properties has been widely analyzed in [5,16].

The basic step of a fast wavelet algorithm is

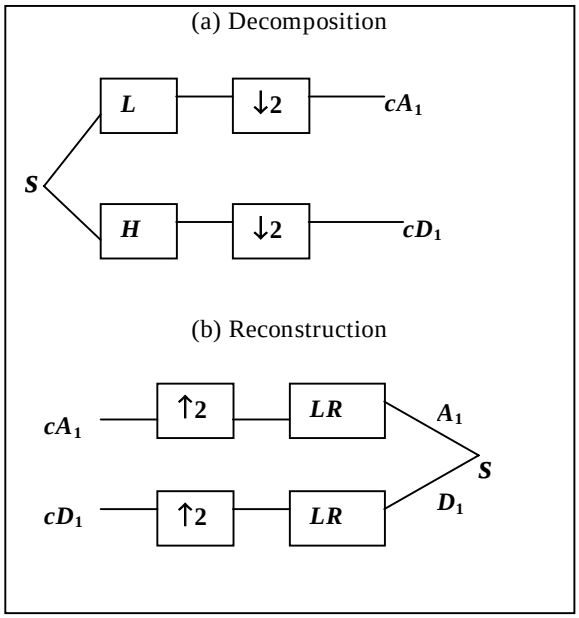

Figure1. Basic step of decomposition and reconstruction of the wavelet transform.

illustrated in Fig.1 and can be implemented in two opposite directions, decomposition and reconstruction. In the decomposition step in Fig. 1(a), the discrete signal s is convolved with a low pass filter L and a high pass filter H, resulting in two vectors cA_1 and cD_1.

The elements of the vector cA_1 are called approximation coefficients and the elements of the vector cD_1 are called detail coefficients. The symbol $\downarrow 2$ denotes downsampling i.e. omitting the odd indexed elements of the filtered signal, so the number of the coefficients produced by the basic step is approximately the same as the number of elements of the discrete signal s. In the reconstruction step in Fig 1(b) a pair of filters LR and HR are convolved with the vectors cA_1 and cD_1 respectively. Two signals are produced resulting in a reconstruction signal A_1 called Approximation, and a reconstruction signal D_1 called Detail. The symbol $\uparrow 2$ denotes upsampling e.g. inserting zeros between the elements of the vectors cA_1 and cD_1. An important property of this step is

$$s = A_1 + D_1 \qquad (3)$$

The procedure of the basic step is repeated on the approximation vector cA_1 and successively on every new approximation vector cA_j. This idea is presented by means of a wavelet tree with J levels, where J is the number of iterations of the basic step. In Fig. 2 the wavelet tree of a wavelet decomposition for J=3 is illustrated. Each vector A_j includes approximately $N_t/2^j$ coefficients, where N_t is the length of the signal s, and provides information about a frequency band $[0, F_S/2^{j+1}]$, where F_S is the sampling rate. The reconstruction signals A_1, D_1 satisfy the equations:

$$A_{j-1} = A_j + D_j$$
$$A_j = \sum_{i \succ j} D_i \qquad (3)$$
$$s = A_j + \sum_{i \le j} D_i$$

where i,j are positive integers.

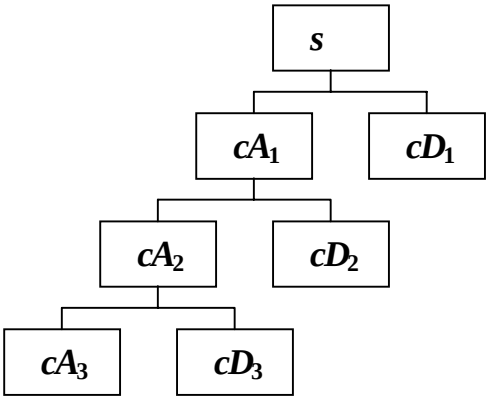

Figure 2. An example of a three level wavelet tree

2.2 The Wavelet Packet Transform (WPT)

The wavelet packet transform is a generalization of the wavelet transform. Let us define two functions $W_0(t)=\varphi(t)$, $W_1(t)=\psi(t)$ where $\varphi(t)$ and $\psi(t)$ are the scaling and wavelet functions respectively. Then in an orthogonal case we can write functions $W_m(t)$, m=0,1,2,…, as

$$W_{2m}(t) = 2\sum_{n=0}^{2N-1} h(n) W_m(2t - n)$$
$$W_{2m+1}(t) = 2\sum_{n=0}^{2N-1} g(n) W_m(2t - n) \qquad (4)$$
$$W_{j,m,n}(t) = 2^{-j/2} W_m(2^{-j}t - n)$$

where j is a scale parameter and n is a time localization parameter. The analyzing functions $W_{j,m,n}$ are called wavelet packet atoms.

In practice a fast algorithm is applied by using the basic step of Fig.1. The difference is that both details and approximations are split into finer components, resulting in a wavelet packet tree. In Fig.3 an example of a wavelet packet decomposition tree of three levels is illustrated. It is observed that the wavelet tree (dashed line) is part of the wavelet packet tree. Each node of the WP tree is indexed with a pair of integers (j,k), where j is the corresponding level of decomposition and k is the order of its position in the specific level. In each level j there are 2^j nodes and their order is k=0,1,…,2^j-1. A vector of wavelet packet coefficients $c_{j,k}$ corresponds to each node (j,k), according to the basic step procedure. The length of a vector $c_{j,k}$ is approximately $N_t/2^j$. From each vector $c_{j,k}$, a reconstruction signal $R_{j,k}$ of length N_t can be produced, by setting to zero the coefficients of all the other vectors in level j, and by

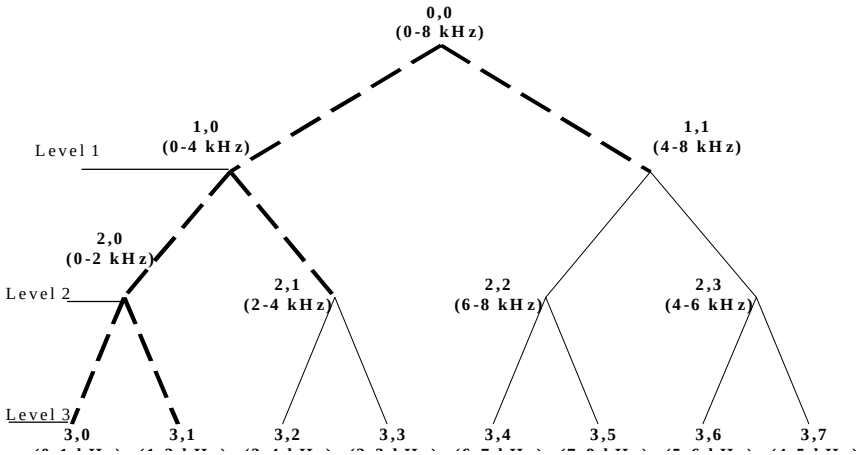

Figure 3. An example of a three level wavelet packet decomposition tree

implementing the wavelet packet tree inversely. The

width of the frequency range corresponding to each reconstruction signal $R_{j,k}$ is $F_j \approx F_S/2^{j+1}$. In Fig.3 the frequency range corresponding to each node of the wavelet packet tree is shown. The sampling rate F_S of the signal is assumed 16 kHz. It is observed that the natural order of the reconstruction signals $R_{j,k}$ in a level j, is not the same as the increasing frequency order. This is explained by the fact that lowpass filters may carry information about high frequency content of the signal, due to frequency folding, caused by downsampling. For example in the third level of the WP tree of Fig.3, the natural order is k=0,1,2,…,7, but the frequency order is k=0,1,3,2,6,7,5,4. The frequency order is denoted by the index p e.g. the vectors $c_{j,p}$ p=0,1,…, 2^j-1 are ordered in frequency order in the level j.

3 The Diagnosis Procedure

The objective of this method is to locate the impact generated transient components of the signal. The successive impacts produce a series of impulse responses, which may be amplitude modulated as a result of the passage of the fault through the load zone or of the varying transmission path between the impact point and the vibration measurement point. The spectrum of such a signal would consist of a harmonic series of frequency components spaced at the bearing defect frequency with the highest amplitude around the resonance frequency. These frequency components are flanked by sidebands if there is an amplitude modulation

The characteristic defect frequencies of a bearing depend on the rotor frequency F_R. For example the BPFI (Ball Pass Frequency Outer Race) of a bearing is rF_R, where r is a constant, which depends on the geometrical characteristics of the bearing. The values of r are known for each type of bearing and in a general case r=10 is proposed as an approximation.

Let us assume that the acceleration signal, measured on a bearing with a defect, is decomposed at J levels. In the J^{th} level, 2^J vectors $c_{J,k}$(i) are produced, where k=0,1,…, 2^J–1 and i=1,…,I. Each vector contains approximately $I=N_t/2^3$ coefficients, and conveys information about a specific frequency band of the signal. The width F_J of each band is approximately $F_J = F_S/2^{J+1}$. In order to diagnose the modulation effects the width of each band should be F_J >3BPFI. Thus, the final level J_f should satisfy:

$$J_f \le \log_2 \frac{F_S}{3rF_R} - 1 \qquad (5)$$

Practically values of J_f=3,4 are appropriate for a great number of signals.

In order to estimate the useful information carried by each vector, several criteria exist, based usually on cost functions, such as the number above a threshold, concentration, entropy, logarithm of energy.

For the purpose of fault diagnosis, the energy of the coefficients above a threshold is used, as a criterion for the selection of the best vector. This idea is based on the fact that the impact components of the signal generate large coefficients in the vectors which correspond to resonance frequency ranges. Besides the coefficients generated by random noise are mainly below a threshold. The selection of a proper threshold is not easy, but in this case it does not affect the resulting signal directly, because this criterion is used only for the selection of the best vector (and consequently frequency band) and no thresholding is applied on the coefficients for the final reconstruction. The procedure of the method is described as follows.

Step 1. The signal s is decomposed at a level J, 2^J vectors $c_{J,k}(i)$ of wavelet packet coefficients are produced. The value of J must be lower than the value of J_f computed by relation (5). Generally J=3 is proposed. The basic idea is that wavelet analysis at deeper levels reduces the time resolution, and the energy of the signal is condensed in fewer coefficients. This is an advantage if the purpose of wavelet analysis is signal compression. For impact generated transient signal feature extraction, proceeding to very deep levels and reducing time resolution might not be effective. Besides, developing the wavelet packet tree up to lower values of J, results in less computational effort. Because of these facts, after level J=3, continuation of decomposition is restricted according to a criterion described in step 5.

Step 2. The mean m and the standard deviation σ of the set of the absolute values of all the coefficients of the vectors $c_{J,p}(i)$ are computed

$$m = \frac{1}{I(2^J-1)} \sum_{p=1}^{2^J-1} \sum_{i=1}^{I} \left| c_{J,p}(i) \right| \qquad (6)$$

$$\sigma = \left[\frac{1}{I(2^J-1)} \sum_{p=1}^{2^J-1} \sum_{i=1}^{I} \left(\left| c_{J,p}(i) \right| - m \right)^2 \right]^{\frac{1}{2}} \qquad (7)$$

The coefficients of the first vector $c_{J,0}(i)$ are omitted because they carry information about low frequencies where discrete harmonics are usually observed due to factors such as unbalance, misalignment etc.

Step 3. In each vector of level J, the coefficients below a threshold t_{hr} are set to zero.

$$t_{hr} = m + \sigma$$
$$\left|c_{J,p}(i)\right| \le t_{hr} \rightarrow c_{J,p}(i) = 0 \quad (8)$$

The thresholded vectors are denoted by $C_{J,p}(i)$.

Step 4. An energy vector $E_J(p)$ is computed

$$E_J(p) = \sum_{i=1,\ldots,I} C_{J,p}(i)^2 \quad (9)$$

Step 5. Let w be the value of p for which

$$E_J(w) = \max(E_J(p)), p = 1,\ldots,2^J - 1 \quad (10)$$

The analysis is continued only for vectors satisfying the relation:

$$E_J(p) > \frac{E_J(w)}{K_{dif}} \quad (11)$$

The parameter K_{dif} is chosen between 1.5 and 2 and adjusts the difficulty of continuation of the decomposition process. If w is the only value of p which satisfies relation (11), the wavelet packet analysis stops and the step 6 is implemented. Otherwise the vectors $c_{J,p}$ corresponding to values of p satisfying relation (11), are further analyzed, implementing the procedure of the basic step of the wavelet packet analysis. In the next level J+1, the steps 2 to 5 are repeated.

Step 6. At the final level J_f the vector $c_{Jf,w}$ corresponding to w as defined in equation (10) is selected as the best. The corresponding reconstruction signal $R_{Jf,w}$ is computed. For the computation of the reconstruction signal $R_{Jf,w}$, only the path from the corresponding node to the starting point of the wavelet packet tree, is necessary to be implemented.

Step 7. The spectrum of the envelope of the reconstructed signal $R_{Jf,w}$ is inspected. A defect is identified by the presence of a characteristic defect frequency and its harmonics. The envelope is estimated based on the Hilbert transform. Alternatively the signal $R_{Jf,w}$ may be rectified by squaring, and FFT-transformed. The rectification generates sum and difference frequencies as well as double frequencies. The difference frequencies dominate the low frequency region of the spectrum of the rectified signal. If modulation exists, the modulating frequencies will be observed. Masking effects will not appear normally, due to the fact that the low frequency region of the signal has been eliminated by omitting the first vector $c_{J,0}(i)$ in the steps 2-5 of the procedure. A problem might occur if the signal $R_{Jf,w}$ corresponds to a vector $c_{Jf,w}$, which is last in the frequency order p of the hypothetically fully decomposed level J_f. Then the frequency content of the signal $R_{Jf,w}$ is near the Nyquist rate and its sum and double-frequency components might fold back to the low frequency range of the rectified signal.

The wavelet db12 of the Daubechies family dbN, is used for wavelet packet analysis [16]. The support length of the functions ψ and φ of these wavelets is 2N-1. Wavelets corresponding to greater values of N, result in better localized frequency ranges corresponding to each node of the wavelet packet tree, but also result in greater computational effort. The wavelet db12 is used as a compromise between accuracy and computational cost. Figure 4 illustrates the automatic diagnosis procedure.

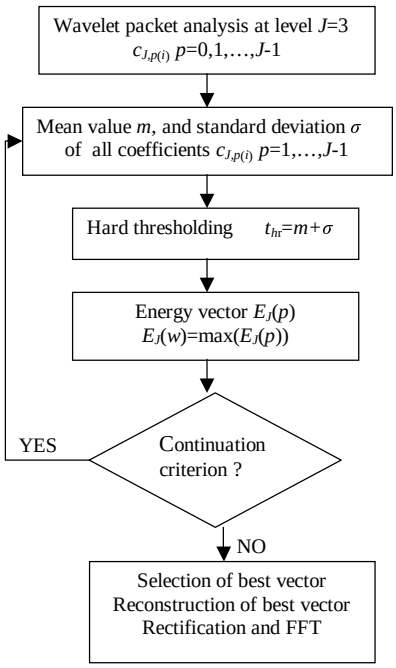

Figure 4. The automatic diagnosis procedure

4 Experiments

The method is first tested on a simulated impulse train. Each impulse is assumed to be modulated by a single harmonic frequency with an exponential decay. This signal can be considered as a simulation of a signal resulting from a rolling element bearing with a fault on the outer race. The impact repetition frequency (BPFO) is assumed to be 120 Hz and the natural frequency excited is assumed to be 3 kHz The sampling rate is assumed 16384 Hz. The resulting simulated waveform, is shown in Fig. 5(a). Figure 5(b) presents the signal after adding a significant level of white Gaussian noise, and two discrete frequencies 20 Hz and 130 Hz in order to simulate low frequency effects. In Fig.6, a) the spectrum of the simulated noisy signal and b) the spectrum of its envelope are illustrated. The impulse sequence information is masked by the low frequency difference (110 Hz) and by the noise. The

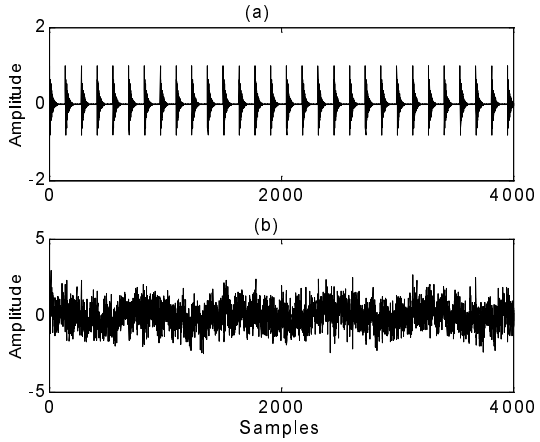

Figure 5. a) A simulated fault pulse sequence. b) The pulse sequence after adding noise and discrete low frequencies.

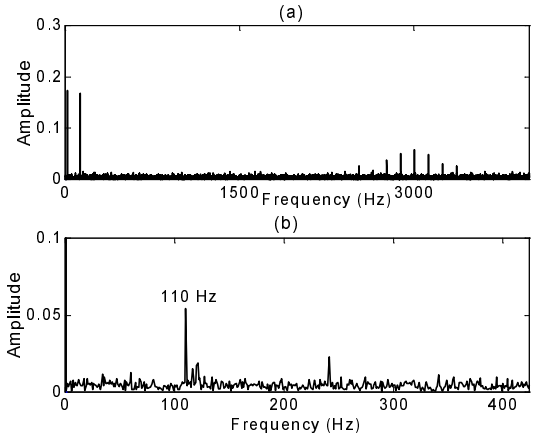

Figure 6. a) Spectrum of the simulated signal of Fig. 5(b). b)The spectrum of the envelope of the signal of Fig.5(b).

proposed procedure is applied up to the third level. In Fig.7 (a) the variation of the energy $E_3(p)$ with respect to the frequency order $p=1,\ldots,7$ of the vectors $c_{3,p}$ of the third level of the wavelet packet tree is illustrated. The maximum value of $E_3(p)$ is observed for p=2, which corresponds to a frequency band containing the assumed resonant frequency 3 kHz. The vector $c_{3,2}$ is selected as the best vector and the corresponding reconstruction signal $R_{3,2}$ is computed. In Fig.7 (b) the spectrum of the rectified signal is shown. It is dominated by the assumed repetition frequency of the impacts (=120 Hz) and its harmonics. The interesting diagnostic information has been detected.

Two characteristic experimental cases are also presented, each one been typical of a vibration response, corresponding to a different type of bearing fault. In all cases, the measuring device was

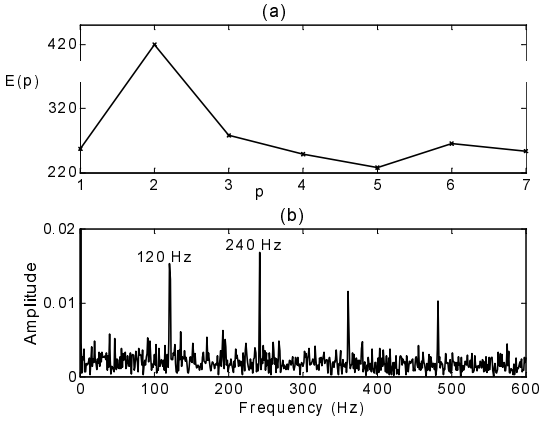

Figure 7. a) Energy of the thresholded vectors in level 3 of the WP tree of the simulated signal, with respect to the frequency order p (step 4). b) The spectrum of the rectified signal obtained in steps 6-7.

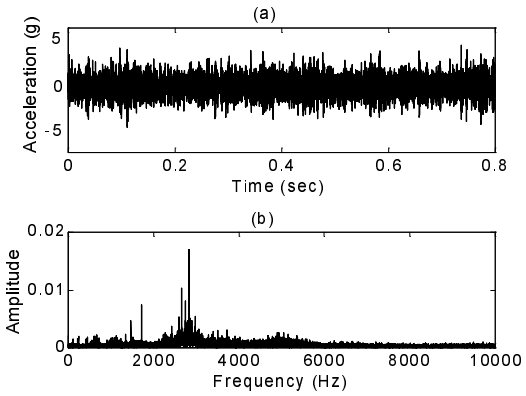

Figure 8. a) Time waveform and b) spectrum, of a vibration signal measured on a bearing with outer race fault.

based on a Pentium II/266MHz portable computer, equipped with a PCMCIA DAQCard-1200 data acquisition card from National Instruments. This is an 8-channel software-configurable 12-bit data acquisition card, with a total sampling rate capacity of 100KHz. A B&K type 8325 accelerometer was used, with a sensitivity of 97.3 mV/g and a dynamic range of 1 Hz to 10 kHz. The code of the algorithm that was used in the data acquisition procedure has been developed under the LabVIEW programming environment of National Instruments. Case A presents an outer race fault and case B an inner race fault. The measurement in case A was conducted on an industrial motor bearing and in case B the measurement was conducted on a machinery fault simulator.

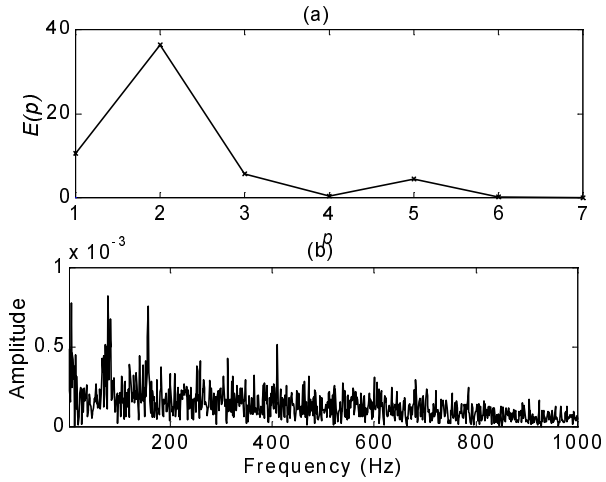

Figure 9. a) Energy of the thresholded vectors in level 3 of the WP tree of the outer race fault signal, with respect to the frequency order p (step 4). b) The spectrum of the rectified signal obtained in steps 6-7.

The bearing examined in Case A is of type 6324MC3 manufactured by SKF. The rotor speed is about 1,500 rpm and the characteristic Ball Passing Frequency Outer race (BPFO) is approximately 78 Hz. The sampling frequency of the measurment was 20 kHz. Figure8 presents (a) the measured acceleration signal and (b) the spectrum of the measured signal. The proposed procedure is applied up to the third level. In Fig.9 (a) the variation of the energy $E_3(p)$ with respect to the frequency order $p=1,\ldots,7$ of the vectors $c_{3,p}$ of the third level of the wavelet packet tree is illustrated. A clear maximum value of $E_3(p)$ for p=2 is observed. The vector $c_{3,2}$ is selected as the best vector and the corresponding reconstruction signal $R_{3,2}$ is computed. The signal $R_{3,2}$ is rectified and its spectrum is shown in Fig.9(b). The BPFO and its first harmonic are observed. The interesting diagnostic information again has been detected.

The bearing examined in Case B consists of 8 balls, has a ball diameter equal to 0.2813 inches, a pitch diameter equal to 1.1228 inches and a contact angle equal to 0 deg. A fault on the inner race was produced. The shaft rotation frequency was about 36 Hz. The sampling frequency of the measurement was 16394 Hz. Figure 10 presents a part of the measured signal. Although a "spiky" behavior is observable in the signal, the nature of the fault cannot be identified without further processing. The proposed method is applied and proceeds up to the fourth level, due to the existence of three resonances as it is observed in the spectrum in Fig10(b). The resulting wavelet packet tree is shown in Fig.11. The vector corresponding to the node (4,10) is selected

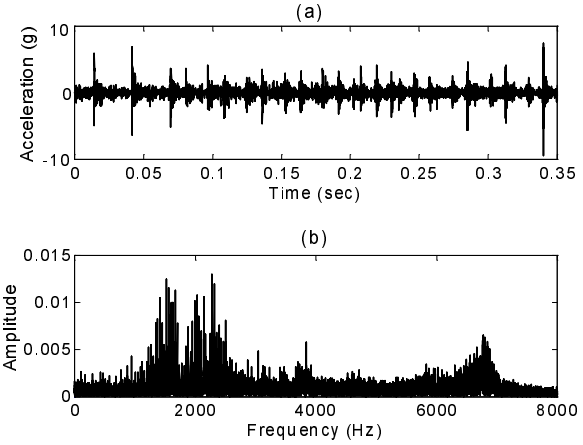

Figure 10. a) Time waveform and b) spectrum, of a vibration signal measured on a bearing with inner race fault.

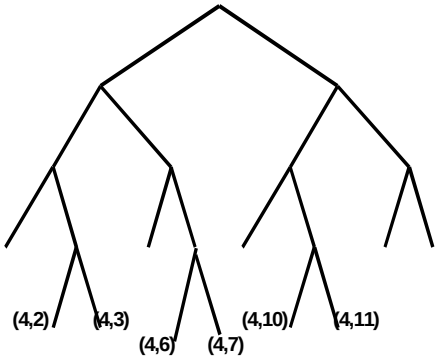

Figure11. Wavelet packet decomposition tree of the inner race fault signal.

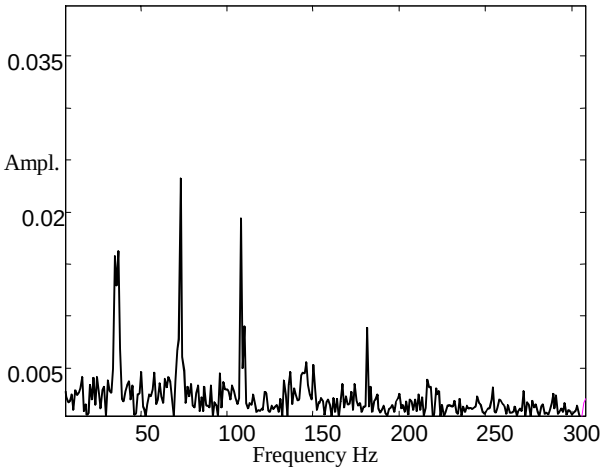

Figure12. Spectrum of the rectified reconstruction signal, obtained by implementation of the WP decomposition tree of Fig.11.

as the best vector after application of the criterion of step 5. Reconstruction and rectification is implemented according to step 7. In Fig.12, the spectrum of the resulting signal is illustrated. The shaft rotation frequency, its harmonics, and the characteristic defect frequency (BPFI=181Hz) are dominating the spectrum. In this case, a strong modulation effect by the shaft rotation frequency is observed, indicating a severe inner race defect.

5 Conclusion

The exploitation of the underlying physical concepts of the modulation mechanism and of the time-frequency localization capabilities of the wavelet packet transform, can lead to an effective method being able to effectively identify the nature of rolling element bearing faults. In all cases, the reconstruction signal obtained, contained the corresponding necessary diagnostic information. Compared to other methods using filters or continuous wavelet transform, it has the advantage of flexibility and efficient computational implementation. A disadvantage is the reduced time resolution in deeper levels of the wavelet packet tree.

The criteria proposed for the selection of the critical parameters of the method perform well and in accordance to the physical parameters of the signals tested. This fact indicates that the implementation of the method can be conducted in an almost automatic way, with the minimal possible degree of user intervention.

References:

[1] N. Tandon, A. Choudhury, A review of vibration and acoustic measurement methods for the detection of defects in rolling element bearings, *Tribology International*, Vol.32**,** 1999, pp. 469-480.

[2] P.D. McFadden, J.D. Smith, Model for the Vibration produced by a single point defect in a rolling element bearing, *Journal of Sound and Vibration*, Vol.96, No.1, 1984, pp. 69-82.

[3] R.B. Randall, *Frequency Analysis*, 3rd Ed, Bruel & Kjaer, 1987

[4] D. Ho.,. R. B Randal, Optimisation of bearing diagnostic techniques using simulated and actual bearing fault signals, *Mechanical systems and Signal Processing*, Vol.14, No.5, 2000, pp. 763-788.

[5] G. Strang, T. Nguyen, *Wavelets and Filter Banks*, Wellesley-Cambridge Press, 1996.

[6] D.E. Newland, *An Introduction to Random Vibration, Spectral and Wavelet Analysis*, Harlow, Longman, 1993

[7] J.C. Li, J. Ma, Wavelet decomposition of vibrations for detection of bearing-localized defects, *NDT&E International***,** Vol.30, No.3, 1997, pp.143-149.

[8] K. Mori, N. Kasashima, T. Yoshioka and Y. Ueno, Prediction of spalling on a ball bearing by applying the discrete wavelet transform to vibration signals, *Wear***,** Vol. 195, 1996, pp. 162-168.

[9] W.J Wang, P.D. McFadden, 1996, Application of wavelets to gearbox vibration signals for fault detection, *Journal of Sound and Vibration***,** Vol.192, No.5, pp. 927-939.

[10] P. D McFadden, J. G. Cook and L. M. Forster, Decomposition of gear vibration signals by the generalized S transform, *Mechanical Systems and Signal Processing*, Vol.13, No**.**5, 1999, pp. 691-707.

[11] J. Lin., L. Qu, Feature extraction based on Morlet wavelet and its application for mechanical fault diagnosis, *Journal of Sound and Vibration*, Vol.234 No.1, 2000, pp.135-148.

[12] D. Donoho, De-noising by soft-thresholding, *IEEE Transactions Inform Theory*, Vol.41, 1995, pp. 612-627.

[13] M. Nielsen, Walsh-Type Wavelet Packet Expansions, *Applied and Computational Harmonic Analysis*, Vol.9, 2000, pp. 265–285.

[14] Y. Wu, R. Du, Feature extraction and assessment using wavelet packets for monitoring of machining processes, *Mechanical Systems and Signal Processing*, Vol.10, No.1, 1996, pp.29-53.

[15]. L. Xiaoli, Y. Zheyun, Toolwear monitoring with wavelet packet transform-fuzzy clustering method, *Wear*, Vol.219, 1998, pp. 145-154.

[16] I. Daubechies, *Ten lectures on wavelets*, SIAM, 1992.